

# Fractals and dynamical chaos in a random 2D Lorentz gas with sinks

I. Claus,<sup>1</sup> P. Gaspard,<sup>1</sup> and H. van Beijeren<sup>2</sup>

<sup>1</sup> *Center for Nonlinear Phenomena and Complex Systems, Faculté des Sciences,  
Université Libre de Bruxelles, Campus Plaine, Code Postal 231,  
B-1050 Brussels, Belgium*

<sup>2</sup> *Institute for Theoretical Physics, Utrecht University,  
Leuvenlaan 4, 3584 CE Utrecht, The Netherlands*

---

## Abstract

Two-dimensional random Lorentz gases with absorbing traps are considered in which a moving point particle undergoes elastic collisions on hard disks and annihilates when reaching a trap. In systems of finite spatial extension, the asymptotic decay of the survival probability is exponential and characterized by an escape rate  $\gamma$ , which can be related to the average positive Lyapunov exponent and to the dimension of the fractal repeller of the system. For infinite systems, the survival probability obeys a stretched exponential law of the form  $P(c, t) \sim \exp(-Ct^{1/2})$ . The transition between the two regimes is studied and we show that, for a given trap density, the non-integer dimension of the fractal repeller increases with the system size to finally reach the integer dimension of the phase space. Nevertheless, the repeller remains fractal. We determine the special scaling properties of this fractal.

*Key words:* Microscopic chaos, escape, repeller.

*PACS:* 05.45.Df, 05.60.-k

---

## 1 Introduction

Many recent works have been devoted to the problem of diffusion in the presence of static absorbing traps, or sinks. In such models, the diffusing particles can be seen as modeling some active chemical species or some kind of excitation. The trapping then consists in a reaction with another chemical species leading to a non-reactive product, or in an excitation trapping converting the energy to some other form [1]. The important quantity to study is the survival probability  $P(c, t)$ , i.e., the probability for a diffusing particle to survive in the system at time  $t$  for a trap concentration  $c$ . In the case of randomly distributed traps, in a system of infinite spatial extension, the survival probability  $P(c, t)$  of the diffusing particles obeys asymptotically a stretched exponential law of the form [2,3]

$$P(c, t) \sim \exp \left[ -A_d u^{2/(d+2)} t^{d/(d+2)} \right], \quad (1)$$

where  $d$  is the dimension of the system,  $c$  is the concentration of static traps,  $u = -\ln(1 - c)$  and  $A_d$  is a constant depending on the dimension and on the geometry of the system. This behavior is due to the existence with a non-vanishing probability of very large trap-free regions in which particles can survive for a very long time [3].

The stretched exponential law (1) has been much studied in stochastic systems although, until now, no study of this phenomenon has been carried out in deterministic chaotic systems. Such a study is of special interest in deterministic chaotic systems where the trapping process is characterized not only by the behavior of the survival probability but also by the fractal set of all the trajectories that never meet a trap. This set is defined in the phase space

of the deterministic system and is referred to as a fractal repeller [4,5].

The fractal repeller associated with the deterministic chaotic diffusion in the presence of *periodically* distributed traps or sinks has been studied in a previous paper [6]. The system studied there was a two-dimensional periodic Lorentz gas: a point particle undergoes elastic collisions on hard disks fixed in the plane and forming a regular triangular lattice. Some of these disks, forming a regular superlattice over the disk lattice, play the role of traps: when the point particle collides on one of them, it is annihilated. In this case, since the size of trap-free regions is bounded, the decay is exponential, characterized by an escape rate  $\gamma$ , so

$$P(c, t) \sim e^{-\gamma t}. \quad (2)$$

The dynamics is chaotic and the repeller has a non-integer fractal dimension.

The purpose of the present paper is to introduce a model for the stretched exponential law (1) which is based on a deterministic dynamics in order to be able to investigate the deterministic features of the process and, especially, the properties of the associated fractal repeller. We might suspect that the fractal dimension of the repeller is integer and equal to the phase space dimension  $D_H = 3$  since, in a random system of infinite spatial extension, the survival probability (1) decays more slowly than the exponential (2). However, if the dimension is integer, a finer characterization of the repeller is required and we might even wonder if the repeller is still a fractal.

In order to find a solution to this puzzle, we first apply the escape-rate formalism to *finite* two-dimensional random Lorentz gases. We confirm that, in such systems, the asymptotic decay is exponential and that the correspond-

ing escape rate can be related to the positive Lyapunov exponent and to the fractal dimension of the fractal repeller.

We next consider *infinite* 2D random Lorentz gases. Thanks to our fast event-driven numerical algorithm and appropriate simulation method, we are able to extend the study of the survival probability to these deterministic chaotic systems.

Finally, we study the transition from finite to infinite 2D random Lorentz gases, which then allows us to determine the evolution of the scaling properties of the fractal repeller when the system size increases and to solve the aforementioned puzzle.

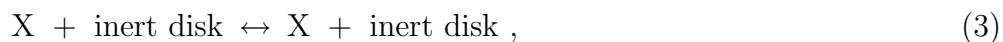
The paper is organized as follows. Section 2 is devoted to finite two-dimensional random Lorentz gases with sinks. The asymptotic decay is shown to be exponential, described by an escape rate  $\gamma$ . Moreover, we show that this open chaotic system is characterized by the existence of a fractal repeller. In these open systems, the average Lyapunov exponent and the fractal dimensions of the repeller are calculated with a non-equilibrium probability measure. The validity of the relation (2) is confirmed for these finite size systems. The case of infinite two-dimensional random Lorentz gases is presented in section 3. Thanks to our appropriate simulation method, the stretched exponential decay is observed for the first time in a deterministic chaotic system. The transition from finite systems with exponential decay to infinite ones obeying stretched exponential laws is studied in section 4. For a given concentration of traps, the Hausdorff dimension of the repeller is shown to increase with system size, to finally reach an integer value equal to the dimension of phase space, as it would be the case for a closed system. We show that, nevertheless, the repeller re-

mains fractal in the infinite-size limit and that it is no longer characterized by a simple power-law scaling as the classical fractals but by a more complicated scaling. Conclusions are drawn in section 5.

## 2 The two-dimensional random Lorentz gas of finite spatial extension

### 2.1 Description of the model

The 2D random Lorentz gas consists of a point particle colliding elastically on randomly and uniformly distributed non-overlapping hard disks fixed in the plane. In finite (or periodic) geometry we will require in addition that the horizon is finite, i.e., that the point particle, starting from any initial condition, collides on a disk after a finite time. Under these conditions the system is diffusive, with a well-defined diffusion coefficient. Some disks are chosen to be sinks: when the point particle collides on one of them, it is absorbed, according to the following reaction scheme:



In practice, we consider a square unit cell of size  $L \times L$ . In this cell,  $n_d$  disks of unit radius are placed randomly in the following way. The disks are first placed periodically, on a square or triangular lattice. A random velocity of unit magnitude is assigned to each of them, and the system is evolved as a hard ball system during a relaxation time  $T_{relax}$ . The configuration is then frozen and  $n_s$  disks are randomly chosen to be sinks. Each disk has the probability  $c$

to be a sink, independently of the others, so  $n_s$  is always close to  $cn_d$ . Three examples of such unit cells are shown in Fig. 1.

The motion of the point particle in the system is defined under periodic boundary conditions. The collisions on the disks are elastic so that the energy of the system is conserved. The magnitude of the point particle velocity is therefore a constant, fixed here to one. The particle velocity can be specified by a unique coordinate, for example the angle  $\psi$  between the velocity and the  $x$ -axis. Its position is specified by two coordinates  $\{x, y\}$ . The three phase-space variables of the point particle are therefore  $\Gamma = \{x, y, \psi\}$ .

## 2.2 *Escape and fractal repeller*

### 2.2.1 *Asymptotic behavior*

To study the asymptotic time behavior in such a system, we define the survival probability  $P(c, t)$ , which is the probability for a point particle to be still in the system at time  $t$ , for a sink concentration  $c$  now taken to be exactly  $n_s/n_d$ . For finite systems in fact this survival probability depends on the positions of the scatterers as well as on the distribution of the traps, but as system size increases the fluctuations of  $P(c, t)$  around its average value will become increasingly smaller. Suppose the long time behavior of  $P(c, t)$  can be written in the form

$$P(c, t) \sim \exp \left[ -C t^{\alpha(t)} \right]. \quad (5)$$

In the case of an exponential decay,  $\alpha$  would be equal to 1, and for the stretched exponential behavior we expect to hold asymptotically in two dimensions, it

would be equal to 0.5. This may be generalized into a time dependent  $\alpha(t)$  defined as [8]

$$\alpha(t) = \frac{d}{d \ln t} \ln[-\ln P(c, t)]. \quad (6)$$

This quantity, obtained numerically, is plotted versus time in Fig. 2.

The first graph, in Fig. 2a, represents the values of  $\alpha$  for the disk configuration represented in Fig. 1a, but with only 4 traps, corresponding to a trap density  $c \approx 0.05$ . An average has been taken over 10 different trap configurations. Figure 2b (respectively 2c) presents the results obtained for the disk configuration of Fig. 1b (respectively 1c), with 5 (respectively 6) traps, corresponding to  $c \approx 0.05$ . In all three cases, we observe that, after a transient,  $\alpha$  slowly tends to 1 [7].

The escape rate characterizing the exponential decay may be obtained as follows [4,5,6]. Let us take  $N_0$  initial conditions randomly distributed in the phase space of variables  $\Gamma = (x, y, \psi)$  according to some initial measure  $\nu_0$ . After a time  $t$ , only a number  $N_t$  of particles will remain in the system. This number will decrease monotonically with  $t$ . The set of particles remaining in the random Lorentz gas at time  $t$  consists of those colliding on a trap, and therefore escaping, at an *escape time*  $\mathcal{T}(\Gamma_0)$ , which is larger than  $t$ :

$$\Upsilon(t) = \{\Gamma_0 : t < \mathcal{T}(\Gamma_0)\}. \quad (7)$$

The decay of the number of particles is expected to be asymptotically exponential due to the finite size of the system. The escape rate is thus defined

as

$$\gamma = \lim_{t \rightarrow +\infty} -\frac{1}{t} \ln \frac{N_t}{N_0} = \lim_{t \rightarrow +\infty} -\frac{1}{t} \ln \nu_0[\Upsilon(t)]. \quad (8)$$

The escape rate is a characteristic quantity of the system, independent of the choice of the initial measure  $\nu_0$  as long as this latter is smooth enough. The escape rate is easily accessible by numerical computations, as shown in Fig. 3. The logarithm of the survival probability is plotted versus time in Fig. 3 for the disk and trap configurations presented in Figs. 1a and c. The behavior is clearly exponential after a short transient. The slopes of the curves give escape rates of  $\gamma = 0.025$  and  $\gamma = 0.017$  respectively.

### *2.2.2 Fractal repeller and nonequilibrium probability measure*

A two-dimensional random Lorentz gas of finite spatial extension with traps is an open system, obeying an asymptotically exponential decay. Moreover, its dynamics is chaotic. It can therefore be studied by the methods developed in Refs. [4,5,6], in order to relate its microscopic chaotic dynamics to its macroscopic exponential decay.

An important property of such a system is the existence of a fractal repeller. For a typical initial condition  $\Gamma_0$ , the particle will collide on a trap and escape after a finite escape time  $\mathcal{T}(\Gamma_0)$ . The same will happen if we follow the trajectory in the negative time direction. Although a forward and a backward escape time exist for almost all trajectories, there do exist trajectories that never collide on a sink and remain trapped forever in the Lorentz gas in both time directions. They can be both periodic and non-periodic. Because of the defocusing character of the collisions on the disks, these non-colliding



trajectories are unstable and form a fractal set of zero Lebesgue measure in phase space: this set is called the fractal repeller  $\mathcal{F}$ . It is a typical feature of chaotic-scattering processes.

Evidence of the fractal character of this repeller is given by the forward escape time  $\mathcal{T}(\Gamma_0)$  as a function of the initial condition, as shown in Fig. 4. This function is finite for almost all initial conditions since the particle typically collides with a sink after a finite time. However, it is infinite for trajectories trapped on the fractal repeller. These trajectories start from initial points on the stable manifold (in the forward direction) of a trajectory that is trapped in both time directions. The infinities of the escape-time function thus establish a fractal set formed by the stable manifold of the fractal repeller,  $W_s(\mathcal{F}_n)$ .

Fig. 4b-d shows this escape time as a function of the initial position, given by an angle  $\theta_0$  around the disk marked by a star in Fig. 4a. The velocity is chosen normal to this disk. Due to the random distribution of disks, the fractal set is not quasi self-similar, as it was the case in Ref. [6]. However, Figs. 4c-d show that a fine structure of escape windows exists at smaller and smaller scale. The characteristics of this structure, such as correlation functions and the distribution of sizes of empty windows, may be expected to show self-similarity on small length scales.

The fractal repeller is the support of an invariant probability measure which can be constructed by considering statistical averages over all the trajectories which have not yet escaped during a time interval  $[-T/2, +T/2]$  and, thereafter, taking the limit  $T \rightarrow \infty$ . In this limit the trajectories which do not escape during  $[0, +T/2]$  have initial conditions on the stable manifold of the repeller,  $W_s(\mathcal{F})$ . On the other hand, the initial conditions of the trajectories

which, in the reverse time direction do not escape during  $[0, -T/2]$  approach the unstable manifold,  $W_u(\mathcal{F})$ . In the limit  $T \rightarrow \infty$ , imposing no escape over the whole interval  $[-T/2, +T/2]$  selects trajectories which approach closer and closer the repeller, given by the intersection  $W_s(\mathcal{F}) \cap W_u(\mathcal{F}) = \mathcal{F}$ . Statistical averages over these selected trajectories define an invariant measure having the fractal repeller for support.

In systems with time-reversal symmetric collision dynamics, such as the present one, statistical averages calculated over the aforementioned invariant measure are equivalent to statistical averages over a conditionally invariant measure defined by selecting the trajectories which do not escape during  $[0, +T/2]$  only and taking the limit  $T \rightarrow \infty$ . This conditionally invariant measure has been constructed in Refs. [4,5,6] and we report the reader to these papers for further detail. Let us here add that, in the limit of low densities of sinks, the system tends to the closed finite Lorentz gas, whereupon the invariant and the conditionally invariant measures reduce to the microcanonical equilibrium measure. In this limit, the escape process stops and the fractal repeller fills the whole phase space.

### *2.2.3 Average Lyapunov exponent of the repeller*

The positive Lyapunov of the repeller can be calculated by averaging over the  $N_T$  particles still in the system after time  $T$  according to

$$\lambda = \lim_{T \rightarrow \infty} \lim_{N_0 \rightarrow \infty} \frac{1}{T} \frac{1}{N_T} \sum_{j=1}^{N_T} \ln \Lambda_T(\Gamma_0^{(j)}), \quad (9)$$

where  $\Lambda_T$  at time  $T$  is the stretching factor of an initial perturbation on the trajectory  $\Gamma_0^{(j)}$  of surviving particles [4,5,6]. The average (9) is equivalent to an

average based on the aforementioned conditional invariant measure as shown in Refs. [4,5].

Numerically, the positive Lyapunov exponent is obtained as the average slope of the logarithm of the stretching factor as a function of time according to Eq. (9). This is illustrated in Figs. 5a and 6a, for the disk and trap configurations depicted respectively in Figs. 1a and 1c. The average Lyapunov exponent respectively equals  $\lambda = 0.75$  and  $\lambda = 1.67$ .

#### 2.2.4 Fractal dimensions of the repeller

Important characteristics of the fractal properties of a repeller are its generalized fractal dimensions. Repellers most often are multifractals, with non-trivial generalized fractal dimensions  $D_q$  [10]. Here the embedding dimension of the repeller is three, since we are working in a 3-dimensional phase space. Therefore, the fractal dimensions of the repeller must satisfy the inequality  $0 \leq D_q < 3$ . Instead of calculating directly the dimensions  $D_q$  of the fractal repeller of the full flow we will consider a set of so-called *partial* fractal dimensions  $d_q$  defined for the intersection of the stable manifold of the repeller  $\mathcal{F}$  with a line  $\mathcal{L}$  across this stable manifold. Like  $\mathcal{F}$  this mostly is a multifractal set. Obviously the values of  $d_q$  must be between 0 and 1. Because the system is time-reversal symmetric the partial dimension in the stable direction is equal to the one in the unstable direction. The direction of the flow contributes a partial dimension equal to unity. Hence for given  $q$ , the dimension  $D_q$  is related to the partial dimension  $d_q$  by  $D_q = 2d_q + 1$ .

In the present paper, we focus on the fractal dimensions for  $q = 0$  and  $q = 1$ .

For  $q = 0$ , we have the *Hausdorff dimension* commonly defined by

$$d_H = d_0 = \lim_{\varepsilon \rightarrow 0} -\frac{\ln N(\varepsilon)}{\ln \varepsilon}, \quad (10)$$

where  $N(\varepsilon)$  is the number of intervals  $I_j$  of equal size  $\varepsilon$ , required to cover the fractal  $f$  defined on a line. For  $q = 1$ , we find the so-called *information dimension*

$$d_I = d_1 = \lim_{\varepsilon \rightarrow 0} \frac{1}{\ln \varepsilon} \sum_{j=1}^{N_I} p_j(\varepsilon) \ln p_j(\varepsilon), \quad (11)$$

where  $p_j(\varepsilon) = \mu(I_j \cap f)$  is the probability weight of the interval  $I_j$  of size  $\varepsilon$ . Here,  $\mu$  denotes the probability measure describing the distribution of points in the fractal set  $f$ . The Hausdorff and information codimensions are defined respectively as  $c_H = 1 - d_H$  and  $c_I = 1 - d_I$ .

For fractal repellers of an open hyperbolic system, a relation exists between the partial information codimension  $c_I$ , the (largest) positive Lyapunov exponent  $\lambda$ , and the escape rate  $\gamma$  [4,5,6]

$$\gamma = \lambda c_I. \quad (12)$$

To a good approximation the information codimension can be replaced by the Hausdorff codimension [4,5]. This last dimension may be calculated with the aid of a numerical algorithm developed by the group of Maryland [4,5,11]. The basic idea of this algorithm is to consider an ensemble of pairs of initial conditions, separated by  $\varepsilon$ , along the line  $\mathcal{L}$  defined above. A pair is said to be uncertain if there is a discontinuity of the escape-time function between both initial conditions. On the other hand, when the pair is certain, the initial conditions belong to an interval of continuity of this function. An estimation of

the fraction of uncertain pairs may be obtained in the following way: typically for an uncertain pair the time after which the pair becomes uncertain coincides with the time that the distance between the points becomes of order unity. This time may thus be estimated as  $t_u = (1/\lambda) \ln(1/\varepsilon)$ . Since trajectories escape at the rate  $\gamma$ , the fraction of uncertain pairs would be proportional to  $\exp(-\gamma t_u) \sim \varepsilon^{\gamma/\lambda} = \varepsilon^{c_I}$ . However, such an estimation needs to be refined to take into account the multifractal character of the repeller and the possibility that  $c_I \neq c_H$  due to local fluctuations of the Lyapunov exponents. A refined estimation of the fraction of uncertain pairs given in the Appendix A for the simple case of a piecewise-linear one-dimensional map shows that

$$f(\varepsilon) \sim \varepsilon^{c_H}, \quad (13)$$

as proved for the general case in Ref. [11]. We notice that, to leading order in the sink density  $c$ , the Hausdorff codimension equals the information codimension [6].

In the case of the Lorentz gas, discontinuities in the escape-time function are not very practical to calculate numerically. Instead one may calculate the fraction of pairs that do not collide with exactly the same sequence of disks until escape from the system. For small  $\varepsilon$  this will behave in precisely the same way as the fraction of uncertain pairs, because it is determined by the same criterion of reaching a distance of order unity between both trajectories of a pair before escaping. The details of the algorithm used here are described in Refs. [4,5].

In Figs. 5b and 6b, the logarithm of the fraction of uncertain pairs (in fact pairs with different collision sequences before escape) is plotted as a function of

the logarithm of the small  $\varepsilon$  separating the two initial conditions of a pair, for the systems defined respectively by the unit cells depicted in Figs 1a and 1c. After a transient regime, the linear behavior confirms the power-law prediction of Eq. (13). The slope gives a value of the Hausdorff codimension equal to  $c_H = 0.034$  and  $c_H = 0.01$  respectively.

For both configurations, the value of the product  $\lambda c_H$  is in good agreement with the value of the corresponding escape rate:  $\lambda c_H = 0.025 = \gamma$  in the former case and  $\lambda c_H = 0.017 = \gamma$  in the latter. Since  $c_H = c_I$  to leading order in the sink density  $c$ , this confirms the validity of the relation (12) for random Lorentz gases of finite spatial extension. This expression connects directly two quantities characterizing the microscopic chaotic dynamics of the Lorentz gas, the average Lyapunov exponent  $\lambda$  and the Hausdorff codimension  $c_H$  of the fractal repeller, and a quantity describing the macroscopic transport behavior of this open system, the escape rate  $\gamma$ .

### **3 The two-dimensional random Lorentz gas of infinite spatial extension**

#### *3.1 Description of the model and simulation method*

We now consider a two-dimensional random Lorentz gas of infinite spatial extension. This supposes that the sinks are randomly distributed among an infinite number of disks. As a consequence, the density of larger and larger trap-free regions decays exponentially with their volume but does not vanish. A suitable method is needed to simulate this situation. It cannot be done with the simple method presented in the previous section: if, in a possibly large,

but in practice always finite system, the nature of the disks is fixed a priori, the size of the largest trap-free region is determined. Trap-free regions of a size that is very rare for the given system size in practice just will not be observed. However, a certain probability  $c$  to be a sink can be assigned to each disk [8,7]. This leads to an average over the different possible sink configurations, as a result of which the probabilities for finding large trap-free regions will attain just the proper values.

Let us define the corresponding configuration-averaged survival probability  $P(c, t)$ , where  $c$  may be interpreted alternatively as the average concentration of sinks. The time evolution of  $P(c, t)$  is given by

$$P(c, t) = \sum_n (1 - c)^n p(n, t) = \langle (1 - c)^{n_t} \rangle \quad (14)$$

where  $n = n_t$  is the number of *different* disks on which the point particle has collided during the time  $t$  and  $p(n, t)$  is the probability that this number is equal to  $n$ .  $\langle \dots \rangle$  is an ensemble average.  $(1 - c)$  is the probability that a disk is not a sink, so that  $(1 - c)^n$  is the probability that none of the disks met at time  $t$  is a sink, in other words the probability that the point particle survives.

To compute the probability  $p(n, t)$  to meet  $n$  different disks in a time  $t$ , a purely deterministic simulation is used. The two-dimensional random Lorentz gas in which the point particle diffuses is defined as in the previous section, by a square unit cell of size  $L \times L$ . Periodic boundary conditions are applied. However, an index is associated with each square cell, allowing us to know which one is currently visited. This is necessary to distinguish one disk from its copies in the other cells. Indeed, if the point particle meets a disk and, later, one of its copies, this should be considered as collisions with different

disks. In other words, although the scatterers are located on a periodic lattice, be it one with a very large unit cell of random filling, the distribution of traps has no periodicity whatsoever.

### 3.2 Theoretical predictions and simulation results

The asymptotic time dependence of the survival probability  $P(c, t)$  is expected to be of the form (1) [2,3,8,12]. For checking this dependence in our system, the easiest method using the idea of Eq. (14) is a direct simulation, in which  $p(n, t)$  is estimated as an average over a large number of uniformly distributed initial conditions. The system considered here has as unit cell the one depicted in Fig. 1c, of size  $25 \times 25$  and with 127 disks. The number of initial conditions is of the order of  $10^8$ .

We present our data following a procedure proposed by Barkema et al. in Ref. [12]. At short times and small concentrations, Eq. (14) can be approximated by [13]

$$P(c, t) = \langle (1 - c)^{n_t} \rangle \simeq (1 - c)^{\langle n_t \rangle}. \quad (15)$$

This is the so-called Rosenstock approximation. In two dimensions,  $\langle n \rangle$  scales as  $4\pi\rho Dt / \ln t$ , with  $\rho$  the average density of scatterers. We therefore expect a time dependence of the survival probability of the form:

$$\begin{aligned} -\ln [P(c, t)] &\sim 4\pi\rho Dt / \ln t \quad \text{at short times and small concentrations,} \\ -\ln [P(c, t)] &\sim (ut)^{1/2} \quad \text{asymptotically,} \end{aligned} \quad (16)$$

with again  $u = -\ln(1 - c)$ . An efficient way to visualize the crossover from one regime to the other is to plot  $-\ln [P(c, t)] / \ln t$  as a function of  $\sqrt{ut} / \ln t$



[12,14]. In the Rosenstock regime, we expect a quadratic dependence, while the stretched exponential regime should produce a linear behavior. The results are represented in Fig. 7 in a double-logarithmic plot. The data collapse for values of  $c$  taken in the range  $[0.01, \dots, 0.09, 0.1, \dots, 0.9]$ . The crossover from a slope 2 to a slope 1 is clear.

The intersection point of the two linear fits gives an estimation of the crossover time from the Rosenstock regime to another regime which ends with the Donsker-Varadhan asymptotics. Using this as reference point, we obtain the dependence on the trap density  $c$  of the crossover time and of the crossover survival probability [12], as presented in Figs. 8a and b respectively. These results show that the crossover occurs at shorter and shorter times and at larger and larger probabilities as the trap density increases. We observe that the crossover probability changes from  $\mathcal{O}(10^{-20})$  to  $\mathcal{O}(10^{-5})$  as the trap density only varies from  $\mathcal{O}(10^{-2})$  to  $\mathcal{O}(1)$ .

A comment is here in order. The extensive numerical simulations of Ref. [15] show that the Donsker-Varadhan behavior is approached only very gradually. It is known to provide an exact asymptote for the logarithm of  $P(c, t)$  including the prefactor of  $(ut)^{1/2}$ . If one inserts the relevant values of the parameters one find this asymptote in Fig. 7 about 20% above the asymptote obtained from the data fit. Given the limited time range over which our numerical data were obtained we may conclude that their behavior is fully compatible with the one observed for stochastic systems in Ref. [15].

## 4 Transition from finite to infinite random systems

We have considered finite random Lorentz gases with exponential behavior and infinite ones with stretched exponential behavior. How does the transition between these two regimes evolve with increasing system size  $L$ ? And what happens to the fractal repeller?

To answer these questions, let us first briefly sketch the arguments of Grassberger and Procaccia for the infinite case [3]. They consider diffusing particles distributed according to a density  $\rho_c(\mathbf{r}, t)$ . The average density  $n_c(\mathbf{r}, t)$  is defined as

$$n_c(\mathbf{r}, t) = \langle \rho_c(\mathbf{r}, t) \rangle_s \tag{17}$$

where  $\langle \dots \rangle_s$  is an average over all the realizations of trap distributions or equivalently over all choices of the origin from which all particles start diffusing initially. A perfectly absorbing sphere of large radius  $R$  centered at the origin is added to the system. The value of the new density  $n'_c(\mathbf{r}, t)$  obtained in the presence of this sphere is necessarily smaller than  $n_c(\mathbf{r}, t)$

$$n_c(\mathbf{r}, t) \geq n'_c(\mathbf{r}, t). \tag{18}$$

$n'_c(\mathbf{r}, t)$  depends on the distribution of traps inside the sphere. If  $\{S\} = \{S_1, S_2, \dots, S_k\}$  are the positions of the traps in the sphere, we have

$$n_c(\mathbf{r}, t) \geq n'_c(\mathbf{r}, t) = \sum_{\{S\}} n'_c(\mathbf{r}, t|\{S\}) P(\{S\}). \tag{19}$$

The sum of the right-hand side can be bounded from below by considering

only one term, corresponding to the situation of a sphere free of traps:

$$n_c(\mathbf{r}, t) > n'_c(\mathbf{r}, t|\{S\} = 0) P(0). \quad (20)$$

A random distribution of sinks corresponds to a Poisson distribution. The probability of finding  $k$  traps in a volume  $v$  is given by

$$P_k = \frac{\bar{N}^k}{k!} \exp(-\bar{N}) \quad (21)$$

with average value  $\bar{N} = n_s v$ , where  $n_s$  is the average density of sinks. The probability to have no trap in the sphere is thus given by  $P(0) = \exp(-C n_s R^d)$ , where  $d$  is the dimension of the system and  $C$  the volume of the unit ball in  $d$  dimensions.

On the other hand,  $n'_c(\mathbf{r}, t|\{S\} = 0)$  is obtained as solution of a diffusion equation of coefficient  $\mathcal{D}_0$  with absorbing boundary conditions on the border of a sphere of radius  $|\mathbf{r}| = R$ . Such a solution is known to decay asymptotically as the exponential  $\exp(-\kappa_d \frac{\mathcal{D}_0}{R^2} t)$ , where  $\kappa_d$  is a constant depending on the dimensionality of the system.

Therefore, Eq. (20) becomes

$$n_c(\mathbf{r}, t) > n'_c(\mathbf{r}, t|\{S\} = 0) P(0) \sim \exp\left(-\kappa_d \frac{\mathcal{D}_0}{R^2} t - C n_s R^d\right). \quad (22)$$

The right-hand side may be maximized as a function of  $R$ , with  $R$  between 0 and  $+\infty$  in an infinite system. This gives us an optimal value for  $R$

$$R = \left(\frac{2\kappa_d \mathcal{D}_0}{dC n_s} t\right)^{1/(d+2)} = \alpha t^{1/(d+2)}. \quad (23)$$

Inserting this result in Eq. (22), one obtains

$$n_c(\mathbf{r}, t) > \exp \left[ -\beta t^{d/(d+2)} \right]. \quad (24)$$

Let us now consider a finite system of linear size  $2L$  with a fixed configuration of traps. As long as  $R = \alpha t^{1/d+2} \ll \left( \frac{\ln L}{n_s} \right)^{1/d}$ , the optimal value of  $R$  is found in a fraction of the volume described by (21) and the stretched exponential behavior is observed. However, for longer times, the maximal value of  $R$  is proportional to  $l_0 \approx (\ln L/n_s)^{1/d}$ . Inserting  $R = l_0$  in Eq. (22) leads to an exponential decay of the form  $\exp \left( -\kappa_d \frac{D_0}{l_0^2} t \right)$ . As  $L$  increases, the time  $t^*$  at which the transition occurs increases.

A logarithmic dependence of  $t^*$  on  $L$  in two dimensions has been proven in Ref. [7].

We now want to study the properties of the repeller. As a preparation, let us first consider the simple one-dimensional map with escape represented in Fig. 9. Starting from the full unit interval at time zero one finds after  $k$  discrete time steps an approximate forward repeller consisting of  $N_k = 2^k$  pieces of sizes  $\varepsilon_k = (1/3)^k$ . The number of pieces is equal to the exponential of the Kolmogorov-Sinai entropy times time,  $N_k = \exp(h_{KS}k)$ , and the linear size of these pieces is given by  $\varepsilon_k = \exp(-\lambda k)$  with the Lyapunov exponent  $\lambda = \ln 3$ . This last equality can be intuitively understood as follows: as time goes on, new structures appear on the repeller on smaller and smaller scales. Therefore, long times correspond to small spatial scales. The total length  $L_k$  of the repeller at time step  $k$  is the product of  $N_k$  and  $\varepsilon_k$ . It decreases exponentially with time as

$$L_k = N_k \varepsilon_k = \exp(h_{KS}k) \exp(-\lambda k) = \exp(-\gamma k), \quad (25)$$

where  $\gamma = \lambda - h_{KS}$  is the escape rate.

The fractal (Hausdorff) dimension of the repeller is thus given by the well-known result

$$D_H = \lim_{\varepsilon \rightarrow 0} \frac{\ln N(\varepsilon)}{\ln \left(\frac{1}{\varepsilon}\right)} = \frac{h_{KS}}{\lambda} = \frac{\ln 2}{\ln 3}, \quad (26)$$

in the illustrative example of Fig. 9. On the other hand, we know that the fraction of uncertain pairs  $f(\varepsilon)$ , as defined for the Maryland algorithm, is proportional to the size  $\varepsilon$  to the power  $C_H$ , with  $C_H$  the codimension of the repeller. From this we obtain

$$f(\varepsilon) \sim \varepsilon^{C_H} \sim \varepsilon^{1-D_H} \sim \frac{\varepsilon}{\varepsilon^{D_H}} \sim \varepsilon N(\varepsilon). \quad (27)$$

Let us now imagine a one-dimensional system in which the escape would obey a stretched exponential law. In this case, the remaining length of the repeller at time  $k$  would obey

$$L_k = N_k \varepsilon_k = \exp(-c k^{1/2}). \quad (28)$$

From the relation  $\varepsilon = \exp(-k \lambda)$ , we can express the time as  $k = \frac{1}{\lambda} \ln \frac{1}{\varepsilon}$ . We get

$$N(\varepsilon) = \frac{L_k}{\varepsilon} = \frac{\exp(-c k^{1/2})}{\varepsilon} = \frac{1}{\varepsilon} \exp \left[ -c \left( \frac{1}{\lambda} \ln \frac{1}{\varepsilon} \right)^{1/2} \right]. \quad (29)$$

From Eq. (27), we have

$$f(\varepsilon) \sim \varepsilon N(\varepsilon) \sim \exp \left[ -c \left( \frac{1}{\lambda} \ln \frac{1}{\varepsilon} \right)^{1/2} \right]. \quad (30)$$

This dependence of the fraction of uncertain pairs on  $\varepsilon$  for a system with

stretched exponential behavior can be tested numerically for the two-dimensional infinite random Lorentz gas, with the help of the Maryland algorithm. The algorithm has to be slightly modified to simulate an infinite system. As mentioned before, the absorbing or non-absorbing nature of the disks is not fixed a priori, but each disk has a probability  $c$  to be a sink. At each collision on a disk, the separation of the pair of particles considered is tested. If separation occurs, the fraction of uncertain pairs is increased by  $(1 - c)^n$ , where  $n$  is the number of *different* disks that the pair has met before separating, so  $(1 - c)^n$  is the probability that the particles have not escaped before separating. Simultaneously, the fraction of escaped pairs is increased by  $[1 - (1 - c)^n]$ . In Fig. 10a, the logarithm of the fraction of uncertain pairs,  $\log_{10} f(\varepsilon)$ , is plotted as a function of the logarithm of the distance between the two initial conditions of the pair,  $\log_{10} \varepsilon$ . In order to check that this curve can be fitted by the expression (30), we plot in Fig. 10b  $\log[-\log_{10} f(\varepsilon)]$  versus  $\log(-\log_{10} \varepsilon)$ . We obtain a linear behavior with slope  $\frac{1}{2}$ , in excellent agreement with Eq. (30).

In the case of a system of finite spatial extension but with high density of disks, as represented in Fig. 1c, we see in Fig. 3b that the transient behavior persists until  $t \simeq 50$ . According to the relation  $\varepsilon = \exp(t\lambda)$ , this corresponds to  $\log_{10} \varepsilon \simeq -34$ . This is consistent with the deviation from the linear curve which is observed in Fig. 6b for large values of  $\varepsilon$ .

In two-dimensional systems like the Lorentz gases we consider here, the codimension appearing in the relation  $f(\varepsilon) \sim \varepsilon^{c_H}$  is a partial codimension, associated with a partial dimension  $d_H$ . The total dimension is given by  $D_H = 1 + 2d_H$ . The total number of small three-dimensional pieces needed to cover

the fractal repeller is given by

$$N(\varepsilon) \sim \frac{1}{\varepsilon} \left[ \frac{f(\varepsilon)}{\varepsilon} \right]^2 \sim \frac{1}{\varepsilon^3} \exp \left[ -2c \left( \frac{1}{\lambda} \ln \frac{1}{\varepsilon} \right)^{1/2} \right]. \quad (31)$$

This type of dependence of  $N(\varepsilon)$  on the size  $\varepsilon$  leads to an integer value of the Hausdorff dimension  $D_H$ . Indeed,

$$D_H = \lim_{\varepsilon \rightarrow 0} \frac{\ln N(\varepsilon)}{\ln \left( \frac{1}{\varepsilon} \right)} = 3 - \lim_{\varepsilon \rightarrow 0} 2c \left( \frac{1}{\lambda} \frac{1}{\ln \frac{1}{\varepsilon}} \right)^{\frac{1}{2}} = 3. \quad (32)$$

This dimension does not contain the information concerning the correction to the power law dependence appearing in Eq. (31). We notice that corrections to a power law also appear for Brownian motion in the plane [16]. In this case, the dependence essentially would take the form

$$N(\varepsilon) \sim \frac{1}{\varepsilon^2} \frac{1}{\ln \ln \frac{1}{\varepsilon}} \quad (33)$$

leading to the integer Hausdorff dimension  $D_H = 2$ .

When the size  $L$  of a finite system with fixed traps increases, the time during which stretched exponential behavior is observed increases likewise, and the range of  $\varepsilon$  over which the fraction of uncertain pairs deviates from a power-law behavior in  $\varepsilon$ . Correspondingly, as seen from Fig. 10, the slope in the linear regime of  $\log_{10} f(\varepsilon)$  versus  $\log_{10} \varepsilon$  becomes smaller and smaller, i.e., the partial Hausdorff codimension of the repeller will be smaller. This means that with increasing  $L$  the Hausdorff dimension of the repeller progressively increases towards the asymptotic value  $D_H = 3$ . The same holds for the information dimension, as in the dominant regions the trap density approaches zero and we saw before that both dimensions approach each other in this limit.

In the case of the two-dimensional random Lorentz gas of infinite spatial ex-

tension, the integer value  $D_H = 3$  of the dimension of the fractal repeller can be understood by intuitive arguments. Indeed, this dimension corresponds to the case of a closed system, without escape. In an infinite system, for a given time  $t$ , there exists with a finite probability a region free of traps of size  $R = \left(\frac{2\kappa_d}{dC} \frac{D_0}{n_s} t\right)^{1/(d+2)}$ . The point particles in this region behave as particles in a closed system until they escape through the “boundary” at  $R$ . As time goes on, larger and larger trap-free regions have to be considered. Even if their density decays exponentially with their size, it does not vanish, so that these regions give the dominant contribution to the measure of the repeller.

Our results show that the repeller is indeed a fractal object in spite of its integer dimension  $D_H = 3$ . This fractality is characterized by the complicated scaling behavior of the fraction (30) of uncertain pairs or of the number (31) of pieces needed to cover the fractal. These theoretical predictions are nicely confirmed by our numerical results.

## 5 Conclusions

We have studied in this paper several types of two-dimensional random Lorentz gases with sinks.

The first model considered is a two-dimensional random Lorentz gas with sinks, of finite spatial extension. In this system, the sinks are randomly distributed among the disks. Due to the finite size of the system, the size of the largest trap-free region is bounded. Therefore, the decay of the number of particles is asymptotically exponential. For this open system, we have shown the existence of a fractal repeller formed by the trajectories that never escape



from the system. Using a non-equilibrium measure on the repeller, we have characterized its chaotic and fractal properties. We have obtained the escape rate  $\gamma$ , the positive Lyapunov exponent  $\lambda$ , and the fractal dimensions of the repeller. A relation between  $\gamma$ ,  $\lambda$ , and the Hausdorff codimension  $c_H$  of the fractal repeller has been numerically tested in the limit of low sink densities. This relation establishes a link between the macroscopic decay and the underlying microscopic chaos.

The second case considered is the two-dimensional random Lorentz gas with sinks, of infinite spatial extension. This situation can be simulated by giving to each disk a certain probability to be a sink, while distinguishing between different periodic images of the same disk. This leads to an average over the different sink configurations. The decay of the survival probability asymptotically obeys the stretched exponential law (1). Here this behavior has been studied numerically for the first time in a deterministic chaotic system.

For a dense 2D random Lorentz gas of finite size  $L$ , the transient stretched exponential regime persists during a time fixed in first approximation by the typical size of the largest trap-free region in the system [see Eq. (23)]. As  $L$  increases, the transient regime is observed for longer and longer times. Simultaneously, the dimension of the repeller increases, reaching the integer value  $D_H = 3$  in the infinite-size limit. We have here been able to show that the repeller remains fractal in the limit and to answer the puzzle mentioned in the introduction by finding the nontrivial scaling property of this plain fractal. Its fractal property can be characterized equivalently by the fraction of uncertain pairs of trajectories starting from initial conditions separated by  $\varepsilon$  or by the number of cells of size  $\varepsilon$  needed to cover the fractal. Both scaling functions show a correction to a simple power law proving that the repeller remains

fractal. The correction depends on the Lyapunov exponent as well as on the exponent  $1/2$  of the stretched exponential law (1) in  $d = 2$ . This nontrivial scaling is remarkably confirmed by our numerical results.

In conclusion, we have been able to show that, in a random deterministic chaotic system of infinite spatial extension with sinks, the repeller composed of all the trajectories that never meet a sink is a plain fractal with special scaling properties related to the stretched exponential decay of the survival probability.

## Acknowledgments

The authors thank Professor G. Nicolis for support and encouragement in this research. IC and PG are supported financially by the National Fund for Scientific Research (F. N. R. S. Belgium). H.v.B. also acknowledges support by the Mathematical physics program of FOM and NWO/GBE.

## A Direct proof that the uncertainty exponent is the Hausdorff codimension

Let us consider the piecewise-linear one-dimensional map:

$$x_{n+1} = \begin{cases} \Lambda_0 x_n & 0 < x_n < A \\ \Lambda_1(1 - x_n) & A < x_n < 1 \end{cases} \quad (\text{A.1})$$

We assign the symbol  $\omega = 0$  to the interval  $[0, A]$  and the symbol  $\omega = 1$  to the interval  $[A, 1]$ .

If  $\Lambda_0, \Lambda_1 > 2$ , almost all the trajectories escape after a finite number of iterations. The subinterval  $I_{\omega_0\omega_1\dots\omega_{n-1}}$  is defined as the set of initial conditions for the trajectories which escape in  $n$  iterations and successively visit the intervals corresponding to the symbolic sequence  $\omega_0\omega_1\dots\omega_{n-1}$ . These subintervals form a partition of the unit interval  $[0, 1]$ :

$$\bigcup_{\omega_0\omega_1\dots\omega_{n-1}} I_{\omega_0\omega_1\dots\omega_{n-1}} = [0, 1] \quad (\text{A.2})$$

The length of the subinterval  $I_{\omega_0\omega_1\dots\omega_{n-1}}$  is

$$\ell_{\omega_0\omega_1\dots\omega_{n-1}} = \frac{K}{\Lambda_{\omega_0}\Lambda_{\omega_1}\dots\Lambda_{\omega_{n-1}}} \quad (\text{A.3})$$

Since the sum of lengths should be equal to one

$$\sum_{n=1}^{\infty} \sum_{\omega_0\omega_1\dots\omega_{n-1}} \ell_{\omega_0\omega_1\dots\omega_{n-1}} = 1 \quad (\text{A.4})$$

the constant  $K$  is given by

$$K = \frac{1 - \Lambda_0^{-1} - \Lambda_1^{-1}}{\Lambda_0^{-1} + \Lambda_1^{-1}} \quad (\text{A.5})$$

and the previously introduced constant  $A$  can now be fixed to the value:

$$A = \frac{1 + K}{\Lambda_0}. \quad (\text{A.6})$$

A pair is uncertain if it falls in a subinterval which is smaller than  $\varepsilon$ . Therefore, the fraction of uncertain pairs is equal to

$$f(\varepsilon) = \sum_{n=1}^{\infty} \sum_{\omega_0\omega_1\dots\omega_{n-1}} \ell_{\omega_0\omega_1\dots\omega_{n-1}} \Big|_{\ell_{\omega_0\omega_1\dots\omega_{n-1}} < \varepsilon}. \quad (\text{A.7})$$

The sum can be reordered in terms of the numbers  $n_0$  (resp.  $n_1$ ) of symbol 0 (resp. 1) in the symbolic sequence  $\omega_0\omega_1\dots\omega_{n-1}$ . We have that  $n_0 + n_1 = n$ .

The fraction of uncertain pairs becomes

$$f(\varepsilon) = \sum_{n_0=0}^{\infty} \sum_{n_1=0}^{\infty} \frac{(n_0 + n_1)!}{n_0! n_1!} \frac{K}{\Lambda_0^{n_0} \Lambda_1^{n_1}} \Big|_{n_0 \ln \Lambda_0 + n_1 \ln \Lambda_1 > \ln(K/\varepsilon)}. \quad (\text{A.8})$$

We use the steepest-descent method for this double sum. The domain of summation is the set of pairs of non-negative integers  $(n_0, n_1)$  above the straight line  $n_0 \ln \Lambda_0 + n_1 \ln \Lambda_1 = \ln(K/\varepsilon)$  in the plane  $(n_0, n_1)$ . The function to be summed decreases exponentially to zero as the exponents  $n_0$  and  $n_1$  tend to infinity above the straight line. Therefore, the sum will be dominated by the maximum of the function on the straight line. If we introduce the alternative variables

$$x_0 \equiv \frac{n_0}{\ln(K/\varepsilon)} \quad \text{and} \quad x_1 \equiv \frac{n_1}{\ln(K/\varepsilon)} \quad (\text{A.9})$$

we thus find

$$f(\varepsilon) \sim \varepsilon \left( \frac{K}{\varepsilon} \right)^D \sim \varepsilon^{1-D} \quad (\text{A.10})$$

with

$$D = x_0 \ln \frac{x_0 + x_1}{x_0} + x_1 \ln \frac{x_0 + x_1}{x_1} \quad (\text{A.11})$$

and the constraint

$$x_0 \ln \Lambda_0 + x_1 \ln \Lambda_1 = 1. \quad (\text{A.12})$$

The maximum of the function is given by the steepest-descent condition

$$\frac{dD}{dx_0} = \ln \frac{x_0 + x_1}{x_0} + \frac{dx_1}{dx_0} \ln \frac{x_0 + x_1}{x_1} = 0. \quad (\text{A.13})$$

With the constraint (A.12), we find that the steepest-descent condition reduces to

$$\ln \Lambda_1 \ln \frac{x_0 + x_1}{x_0} = \ln \Lambda_0 \ln \frac{x_0 + x_1}{x_1}. \quad (\text{A.14})$$

We now show that the exponent  $D$  is equal to the Hausdorff dimension. In the present piecewise-linear map, the Hausdorff dimension of the repeller must satisfy by definition the following condition

$$\frac{1}{\Lambda_0^D} + \frac{1}{\Lambda_1^D} = 1. \quad (\text{A.15})$$

Let us show that it is indeed the case. For this purpose, we first express the quantity  $D$  in terms of  $x_0$  and  $x_1$  by Eq. (A.11). Then, we use the steepest-descent condition (A.14) and, thereafter, the constraint (A.12). The calculations are the following:

$$\begin{aligned} \frac{1}{\Lambda_0^D} + \frac{1}{\Lambda_1^D} &= e^{-x_0 \ln \frac{x_0+x_1}{x_0} \ln \Lambda_0 - x_1 \ln \frac{x_0+x_1}{x_1} \ln \Lambda_0} \\ &\quad + e^{-x_0 \ln \frac{x_0+x_1}{x_0} \ln \Lambda_1 - x_1 \ln \frac{x_0+x_1}{x_1} \ln \Lambda_1} \end{aligned} \quad (\text{A.16})$$

$$= e^{-(x_0 \ln \Lambda_0 + x_1 \ln \Lambda_1) \ln \frac{x_0+x_1}{x_0}} + e^{-(x_0 \ln \Lambda_0 + x_1 \ln \Lambda_1) \ln \frac{x_0+x_1}{x_1}} \quad (\text{A.17})$$

$$= e^{-\ln \frac{x_0+x_1}{x_0}} + e^{-\ln \frac{x_0+x_1}{x_1}} = 1 \quad (\text{A.18})$$

Q.E.D.

The previous calculation provides a direct proof that the uncertainty exponent of the Maryland algorithm is the Hausdorff codimension in a piecewise-linear map with two branches. Consequently, the uncertainty exponent should be expected to differ from the information codimension on general multifractal repellers. Indeed, by using the example (A.1), we have numerically observed that the uncertainty exponent agrees with the Hausdorff codimension but

differs from the information codimension if  $\Lambda_0 \neq \Lambda_1$ .

The direct proof presented here can be extended to piecewise-linear one-dimensional maps with more than two branches. In the case of  $m$  branches, there would be  $m$  variables  $n_i$  or  $x_i$  and  $(m - 1)$  steepest-descent conditions such as (A.13) because of the constraint that the maximum point belongs to the hyperplane  $\sum_{i=1}^m n_i \ln \Lambda_i = \ln(K/\varepsilon)$ . Otherwise, a Lagrange multiplier may be introduced, to deal with this constraint in the search of the maximum. In the general case, the argument of Ref. [11] provides the proof.

## References

- [1] S. Havlin and D. Ben-Avraham, *Adv. Phys.* **36**, 696 (1987), and references therein.
- [2] M. Donsker and S. R. S. Varadhan, *Commun. Pure Appl. Math.* **28**, 525 (1975); **32**, 721 (1979).
- [3] P. Grassberger and I. Procaccia, *J. Chem. Phys.* **77**, 6281 (1982).
- [4] P. Gaspard and F. Baras, *Phys. Rev. E* **51**, 28 (1995).
- [5] P. Gaspard, *Chaos, Scattering, and Statistical Mechanics* (Cambridge University Press, Cambridge UK, 1998).
- [6] I. Claus and P. Gaspard, *Phys. Rev. E* **63**, 036227 (2001).
- [7] A. Bunde, S. Havlin, J. Klafter, G. Gräff, and A. Shefter, *Phys. Rev. Lett.* **78**, 3338 (1997).
- [8] J. K. Anlauf, *Phys. Rev. Lett.* **52**, 1845 (1984).
- [9] Ya. G. Sinai, *Russian Math. Surveys* **25**, 137 (1970).

- [10] T. C. Hasley, M. H. Jensen, L. P. Kadanoff, I. Procaccia, and B. I. Shraiman, Phys. Rev. A **33**, 1141 (1986).
- [11] S. W. McDonald, C. Grebogi, E. Ott, and J. A. Yorke, Physica D **17**, 125 (1988).
- [12] G. T. Barkema, P. Biswas, and H. van Beijeren, Phys. Rev. Lett. **87**, 170601 (2001)
- [13] H. B. Rosenstock, J. Math. Phys. **11**, 487 (1970); J. W. Haus and K. W. Kehr, Phys. Rep. **150**, 263 (1987).
- [14] According to the recent Ref. [15], improved agreement with the asymptotic formulas can be obtained by including non-leading corrections.
- [15] V. Mehra and P. Grassberger, Physica D **168**, 244 (2002).
- [16] B. Mandelbrot, *The Fractal Geometry of Nature* (W. H. Freeman, New York, 1977).

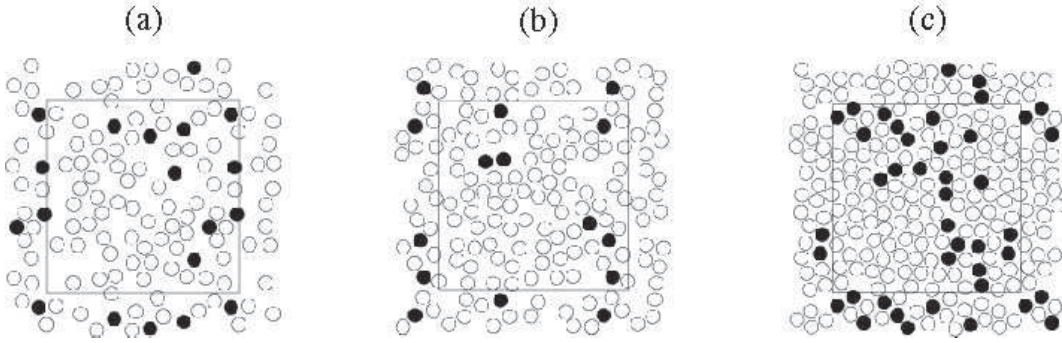
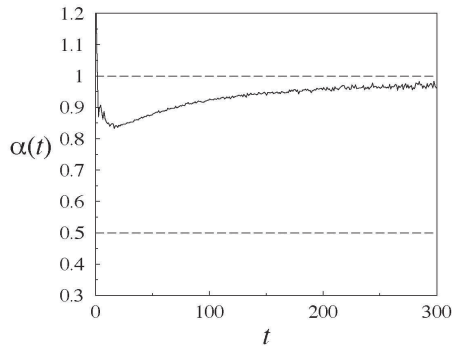
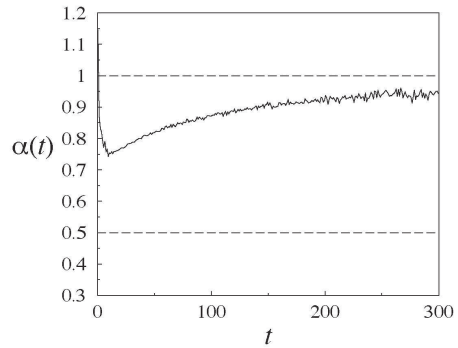


Fig. 1. Typical unit cell of a finite two-dimensional random Lorentz gas: (a)  $L = 25$ ,  $n_d = 72$ ,  $n_s = 9$ ; (b)  $L = 25$ ,  $n_d = 88$ ,  $n_s = 7$ ; (c)  $L = 25$ ,  $n_d = 127$ ,  $n_s = 23$ . The filled disks are the sinks.

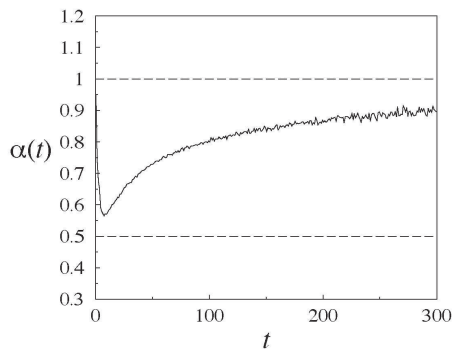




(a)

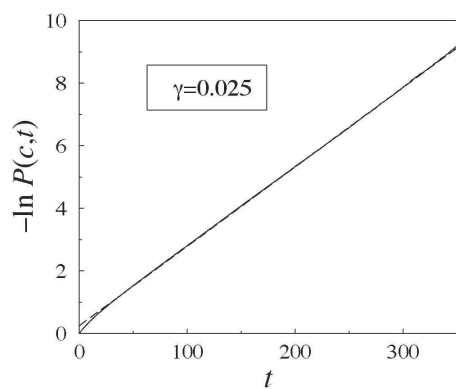


(b)

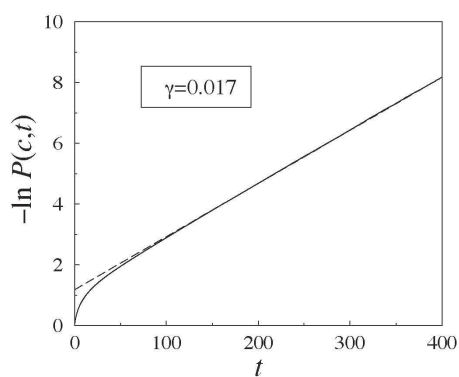


(c)

Fig. 2. Two-dimensional random Lorentz gas of finite spatial extension; Effective exponent  $\alpha$  plotted versus time, for a trap density  $c \approx 0.05$ : (a) in the case of the disk configuration represented in Fig. 1a, but with  $n_s = 4$  traps; (b) in the case of the disk configuration represented in Fig. 1b, but with  $n_s = 5$  traps; (c) in the case of the disk configuration represented in Fig. 1c, but with  $n_s = 6$  traps.

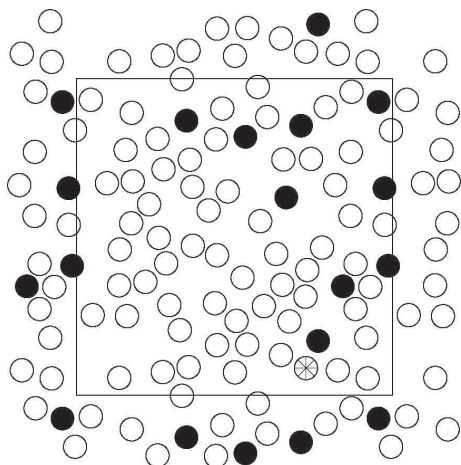


(a)

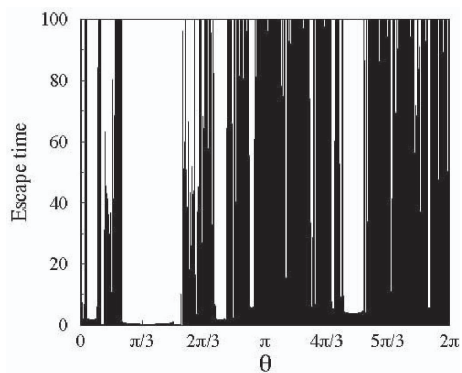


(b)

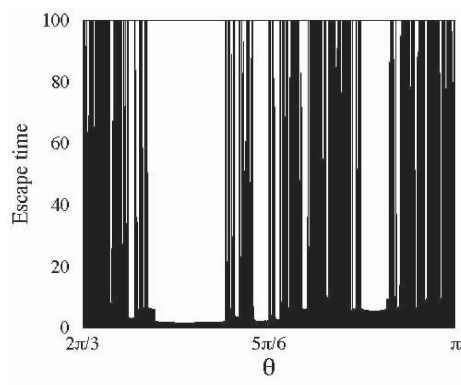
Fig. 3. Two-dimensional random Lorentz gas of finite spatial extension; Logarithm of the survival probability as a function of time: (a) for the disk and trap configuration represented in Fig. 1a, (b) for the disk and trap configuration represented in Fig. 1c. After a transient time the behavior is exponential and the slope of the curve gives the value of the escape rate  $\gamma$ .



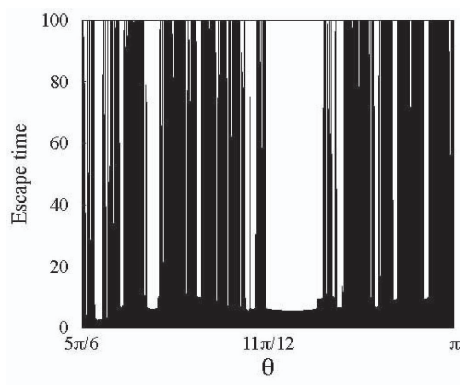
(a)



(b)

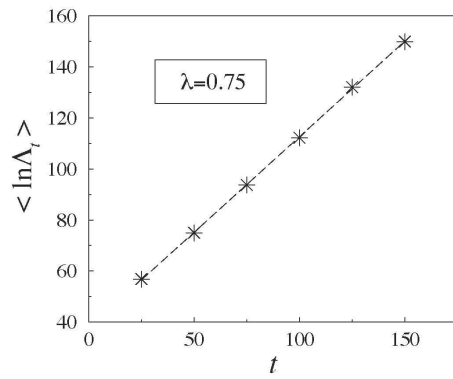


(c)

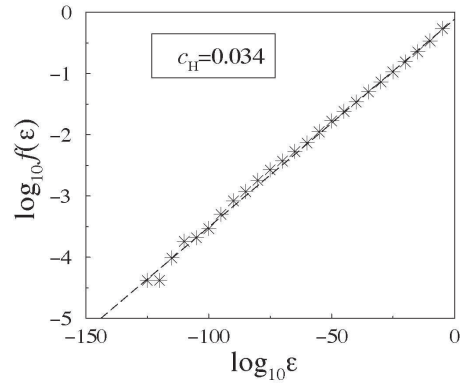


(d)

Fig. 4. Escape time as a function of the initial position: (a) The initial positions are taken at a varying angle  $\theta$  around the disk marked by a star; the initial velocity is always normal to the disk. Escape time for (b)  $\theta \in [0, 2\pi]$ ; (c)  $\theta \in [2\pi/3, \pi]$ ; (d)  $\theta \in [5\pi/6, \pi]$ .

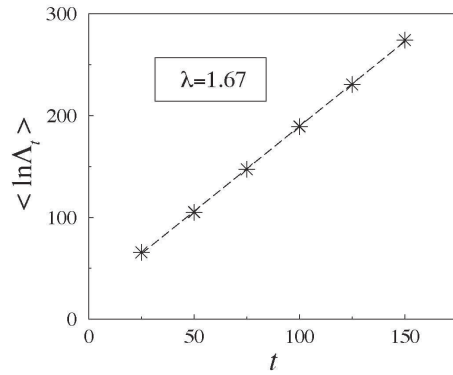


(a)

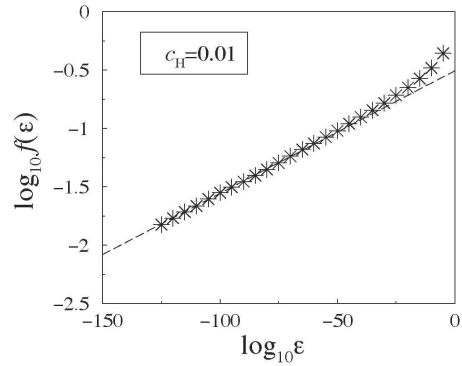


(b)

Fig. 5. Two-dimensional random Lorentz gas of finite spatial extension defined by the unit cell represented in Fig. 1a: (a) Average of the logarithm of the stretching factors, as a function of time  $t$ . The slope gives the average Lyapunov exponent  $\lambda = 0.75$ . (b) Maryland algorithm: the logarithm of the fraction of uncertain pairs as a function of the logarithm of the difference  $\varepsilon$  between the two initial conditions of the same pair. The slope gives the Hausdorff codimension  $c_H = 0.034$ . The product  $\lambda c_H = 0.025$  is in good agreement with the value of  $\gamma$ , obtained from Fig. 3a.



(a)



(b)

Fig. 6. Two-dimensional random Lorentz gas of finite spatial extension defined by the unit cell represented in Fig. 1c: (a) Average of the logarithm of the stretching factors, as a function of time  $t$ . The slope gives the average Lyapunov exponent  $\lambda = 1.67$ . (b) Maryland algorithm: the logarithm of the fraction of uncertain pairs as a function of the logarithm of the difference  $\varepsilon$  between the two initial conditions of the same pair. The slope gives the Hausdorff codimension  $c_H = 0.01$ . The product  $\lambda c_H = 0.017$  is in good agreement with the value of  $\gamma$ , obtained from Fig. 3b.

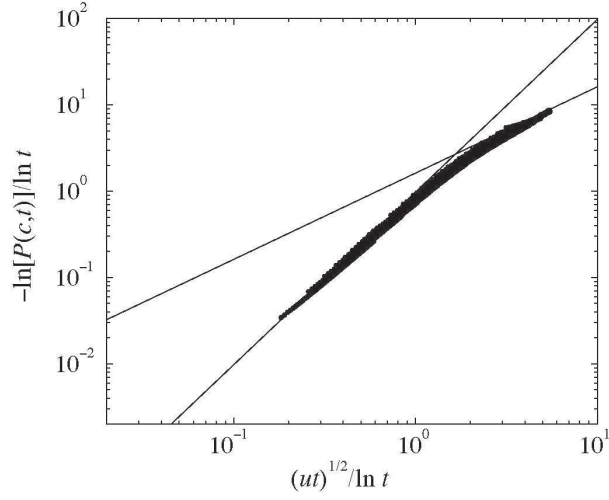


Fig. 7. Infinite two-dimensional random Lorentz gas: Crossover from the Rosenstock regime to the stretched exponential regime.  $-\ln [P(c, t)] / \ln t$  is plotted as a function of  $\sqrt{ut} / \ln t$  in a double logarithmic plot. The solid lines are fits to the data with slopes 2 and 1. They cross at the point (1.7, 2.7).

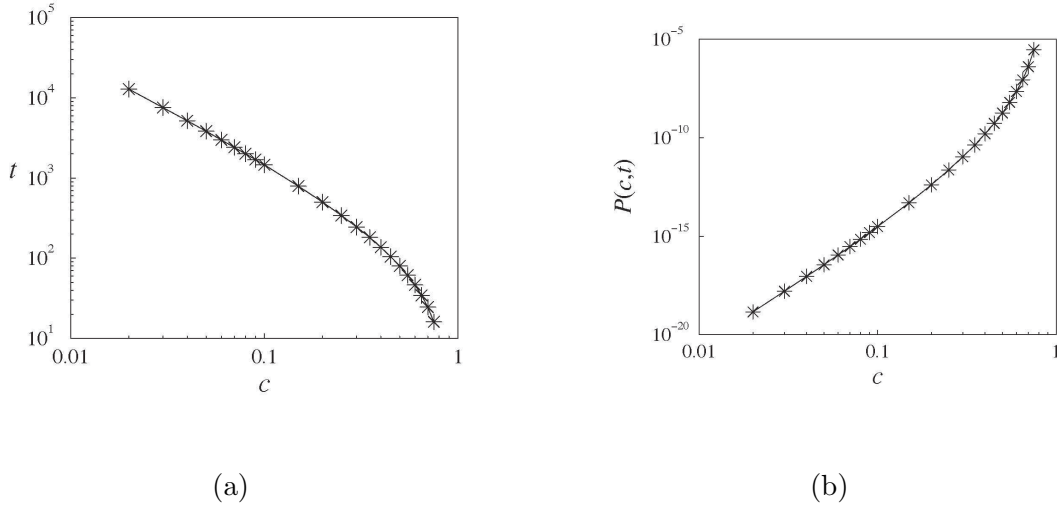


Fig. 8. (a) Crossover time from the Rosenstock regime to the stretched exponential regime as a function of the trap density  $c$ . (b) Dependence of the crossover survival probability on the trap density  $c$ .

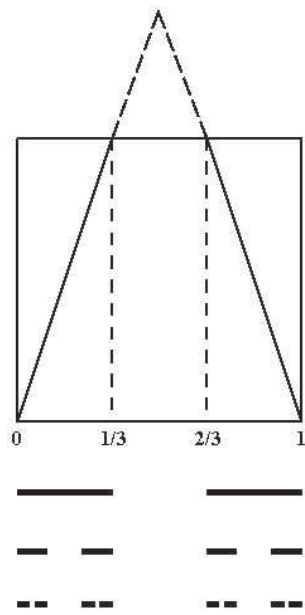
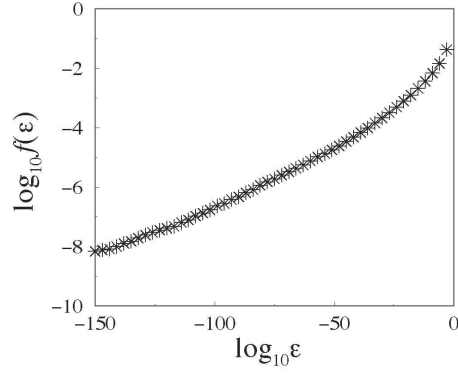
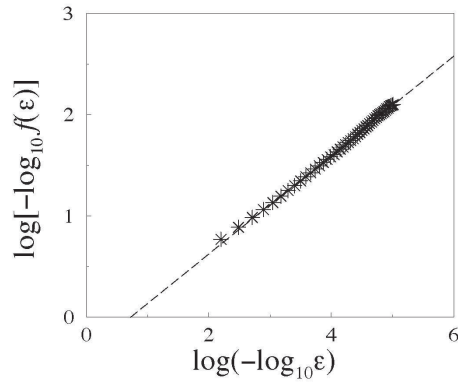


Fig. 9. One-dimensional map with escape.



(a)



(b)

Fig. 10. Maryland algorithm in the case of a random Lorentz gas of infinite spatial extension: the system considered is represented in Fig. 1b, with a sink density  $c = 0.6$ . (a) The logarithm of the fraction of uncertain pairs is plotted as a function of the logarithm of the difference  $\varepsilon$  between the two initial conditions of the same pair. (b) Logarithmic representation of the same quantities, confirming the dependence predicted by Eq. (30).